

DR ZHAO WANG (Orcid ID : 0000-0001-5431-1785)

DR PENG ZHAN (Orcid ID : 0000-0002-9675-6026)

PROFESSOR XINYONG LIU (Orcid ID : 0000-0002-5833-3807)

Article type : Research Article

Design, Synthesis, and Antiviral Evaluation of Novel Hydrazone-substituted Thiophene[3,2-*d*]pyrimidine Derivatives as Potent HIV-1 Inhibitors

Zhao Wang,[†] Dongwei Kang,[†] Meng Chen,[/] Gaochan Wu,[†] Da Feng,[†] Tong Zhao,[†] Zhongxia Zhou,[†] Zhipeng Huo,[†] Lanlan Jing,[†] Xiaofang Zuo,[†] Dirk Daelemans,[§] Erik De Clercq,[§] Christophe Pannecouque,[§] Peng Zhan,^{†,*} and Xinyong Liu^{†,*}

[†] Department of Medicinal Chemistry, Key Laboratory of Chemical Biology (Ministry of Education), School of Pharmaceutical Sciences, Shandong University, 44 West Culture Road, 250012 Jinan, Shandong, PR China

[/] Shandong Center for Disease Control and Prevention, 250014 Jinan, Shandong, PR China

[§] Rega Institute for Medical Research, Laboratory of Virology and Chemotherapy, K.U.Leuven, Herestraat 49 Postbus 1043 (09.A097), B-3000 Leuven, Belgium.

This article has been accepted for publication and undergone full peer review but has not been through the copyediting, typesetting, pagination and proofreading process, which may lead to differences between this version and the Version of Record. Please cite this article as doi: 10.1111/cbdd.13373

This article is protected by copyright. All rights reserved.

ABSTRACT

In the previous studies of our lab, the thiophene[3,2-*d*]pyrimidine was identified as a promising scaffold for seeking highly potent HIV-1 non-nucleoside reverse transcriptase inhibitors (NNRTIs). In the present study, we designed, synthesized, and biologically evaluated a series of thiophene[3,2-*d*]pyrimidine derivatives with changed linker between the thiophenepyrimidine core and the right wing. Some of the synthesized compounds exhibited excellent HIV-1 inhibitory potency with low (double-digit) nanomolar EC₅₀ values. Among them, compound **13a** exhibited the most potent anti HIV-1 activity (EC₅₀ = 21.2 nM), which was 10-fold greater than that of NVP (EC₅₀ = 281 nM). Moreover, **13a** showed much lower cytotoxicity (CC₅₀ = 183 μM) and higher SI (SI = 8632) than NVP, ETV and AZT. Besides, some physicochemical properties and water solubility were calculated or measured. The preliminary structure-activity relationships and molecular simulation studies of these compounds were also discussed comprehensively to provide valuable direction for further design and optimization.

KEYWORDS: HIV-1, NNRTIs, DAPY, thiophene[3,2-*d*]pyrimidine, backbone-binding, molecular simulation

INTRODUCTION

Acquired immune deficiency syndrome (AIDS), which mainly caused by human immunodeficiency virus type-1 (HIV-1), is one of the world's most serious infectious diseases which threaten human's health.¹ HIV-1 reverse transcriptase (RT) is a key target for anti-AIDS drug design for its well-known mechanism and well-solved three dimensional structure.² Non-nucleoside RT inhibitors (NNRTIs) bind to the allosteric binding site (NNRTIs binding pocket, NNIBP) about 10 Å distantly from the polymerase active site of RT, leading to catalytic region's conformational change and contribute to the inhibition of its

DNA polymerase activity.^{1,3} Compared with other inhibitors, NNRTIs have gained an essential place in the highly active antiretroviral therapy (HAART) regimens to treat HIV infection, owing to their unique antiviral potency, relatively low toxicity and high selectivity.⁴ So far, five NNRTIs have been approved for clinical use by US FDA, including first-generation drugs nevirapine (**1**, NVP), delavirdine (**2**, DLV), and efavirenz (**3**, EFV), and second-generation drugs etravirine (**4**, ETV) and rilpivirine (**5**, RPV) (**Figure 1**).^{5,6} However, in view of the emergence of drug-resistance and the mutation of virus (especially K103N/Y181C), the therapeutic efficacies of the first generation of NNRTIs were dramatically downplayed. The second-generation drugs ETV and RPV belong to the diarylpyrimidine (DAPY) family, which comprises the most successful NNRTIs, exhibited broad spectrum of activities against drug-resistant HIV-1 strains, but their low solubility and poor bioavailability limit their clinical use.^{7,8} Therefore, there still remains an urgent need to conduct further modifications based on the DAPY skeleton and develop novel DAPY-based NNRTIs with improved antiviral efficacy and favorable pharmacokinetic profiles.⁹

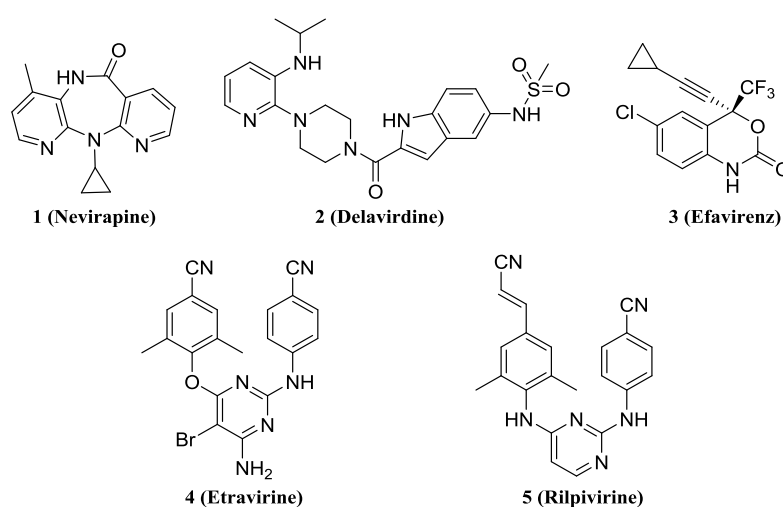


Figure 1. Chemical structures of NNRTIs approved by the US FDA

According to the traditional drug design strategy, a promising NNRTI should enter the NNIBP effectively and occupy the binding pocket maximally, therefore interacting effectively with the amino acids around the binding site, particularly to promote a robust network of hydrogen bonding interactions with backbone atoms of amino acid residues in the NNIBP.¹⁰ Previous research in our lab demonstrated that the piperidine-substituted

thiophene[3,2-*d*]pyrimidine is a promising scaffold of DAPY NNRTIs.^{11–14} It is worth noting that the most potent compound **6** (K-5a2) exhibited a significantly improved drug resistance profile compared to ETV. Molecular docking results showed that **6** could form considerably more direct or water-mediated hydrogen bonding interactions between their polar groups (the thiophene sulfur, piperidine nitrogen and solvent-exposed sulfonamide) and the main chains of amino acid residues throughout the NNIBP.¹¹ This extensive network of main chain hydrogen bonds are less susceptible to side chain mutations in the pocket, which contributes mostly to its improved drug resistance profiles. The research work on **6** further illustrates that the backbone-binding concept is an effective strategy to overcome drug resistance.¹⁴ Therefore, we have continued to apply the backbone-binding design strategy resulting in the design and synthesis of a variety of thiophene[3,2-*d*]pyrimidine derivatives with intriguing structural features.

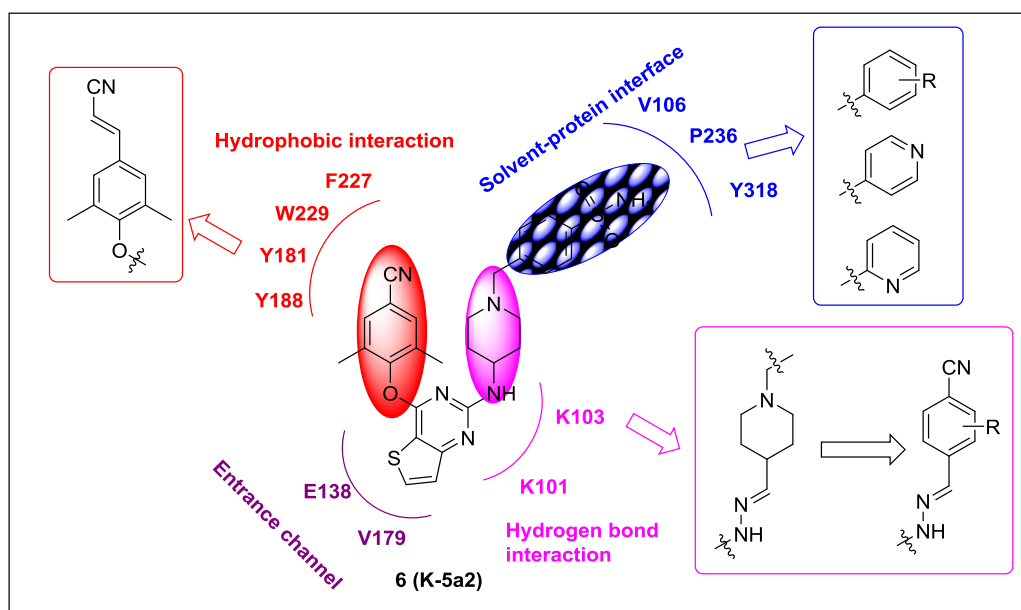


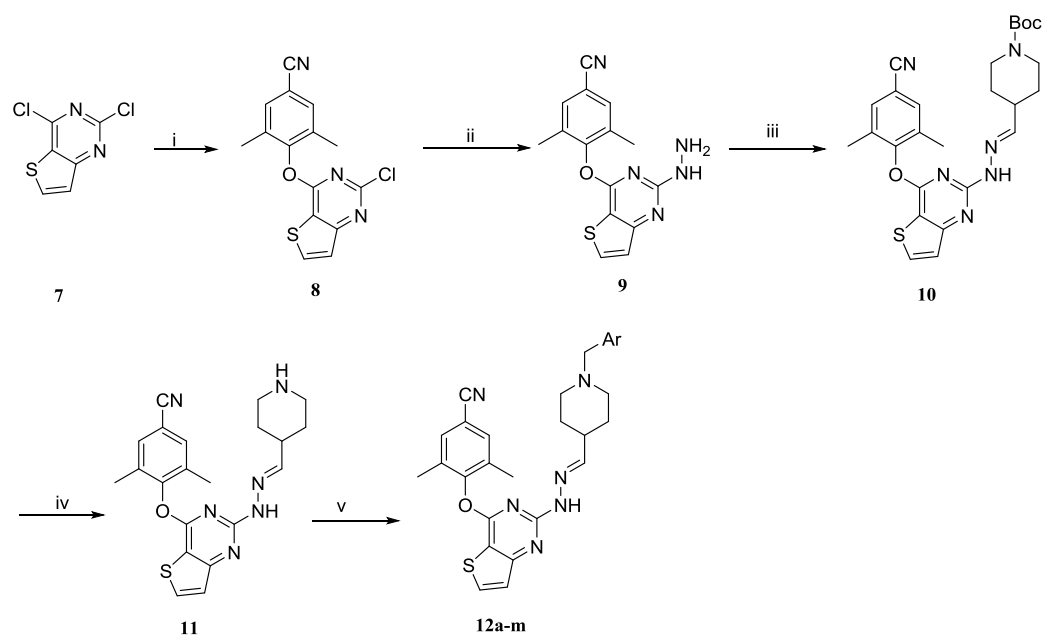
Figure 2. Further structure optimization of thiophene[3,2-*d*]pyrimidine **6**

With **6** as lead compound, we conducted the further structure modification from the following two parts: 1) replacement the *NH* linker connecting the central pyridine ring and the right ring with a hydrazone linker, with the hope that the newly increased *N* atom could develop additional hydrogen bonds with the main chain of Lys103; 2) benzonitrile was introduced to the right wing according to bioisosterism strategy. For the purpose of

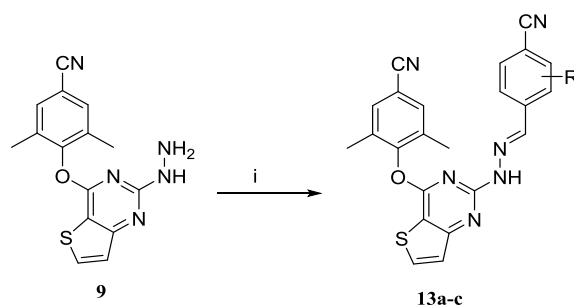
developing more hydrogen bonds with the main chain of Lys103, the fluorine atom was introduced to the C₂ and C₃ position of the benzonitrile. In addition, we also introduced the cyano vinyl group in the left wing, anticipating that it could form stronger hydrophobic interactions with highly conserved amino acid residues (**Figure 2**). Herein we report the synthesis and biological evaluation of these novel compounds. Moreover, preliminary SARs and molecular simulation studies were also discussed to gain further insights into this series of analogues.

CHEMISTRY

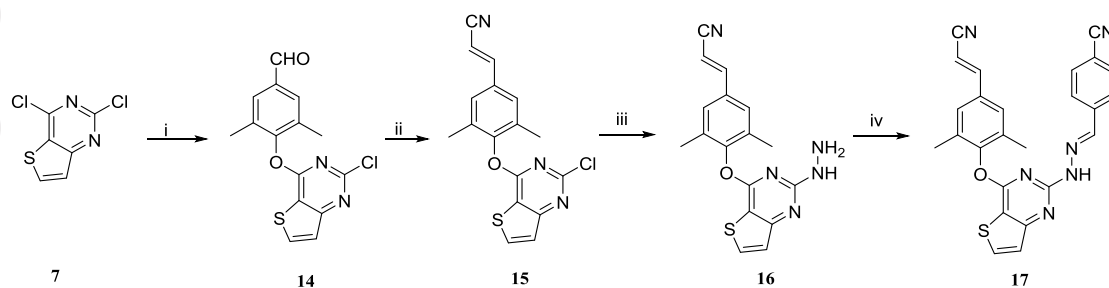
The synthetic routes of the newly designed compounds are outlined in **Schemes 1-3**.^{15,16} In **Scheme 1**, the commercially available 2,4-dichlorothiophene[3,2-*d*]pyrimidine (**7**) was selected as starting material, which engaged in nucleophilic substitution reaction with 3,5-dimethyl-4-hydroxybenzonitrile in the presence of potassium carbonate to afford the intermediate **8**. Then the intermediate **9** was obtained via the hydrazinolysis of **8** in the presence of hydrazine hydrate. **9** was reacted with 1-(tert-butoxycarbonyl)-4-formylpiperidine to afford the intermediate **10**, which was directly deprotected with trifluoroacetic acid to yield **11**. Subsequently, treatment of the intermediate **11** with various substituted aromatic groups in the presence of potassium carbonate yielded the target compounds **12a-m**. The target compounds **13a-c** were prepared by treating **9** with 4-cyanobenzaldehyde or fluorine substituted 4-cyanobenzaldehyde in ethanol.



Scheme 1. Reagents and Conditions: (i) 3,5-dimethyl-4-hydroxybenzonitrile, DMF, K_2CO_3 , r.t.; (ii) 80% hydrazine hydrate, ethanol, reflux; (iii) 1-(tert-Butoxycarbonyl)-4-formylpiperidine, ethanol, reflux; (iv) TFA, DCM, r.t.; (v) substituted benzyl chloride (or bromine) or 2-picolyl chloride hydrochloride or 4-picolyl chloride hydrochloride, DMF, K_2CO_3 , r.t.



Scheme 2. Reagents and Conditions: (i) substituted 4-cyanobenzaldehyde or 4-cyanobenzaldehyde, ethanol, reflux.



Scheme 3. Reagents and Conditions: (i) 3,5-dimethyl-4-hydroxybenzaldehyde, DMF, K₂CO₃, r.t.; (ii) (EtO)₂P(O)CH₂CN, t-BuOK, THF, 0°C to r.t.; (iii) 80% hydrazine hydrate, ethanol, reflux; (iv) 4-cyanobenzaldehyde, ethanol, reflux.

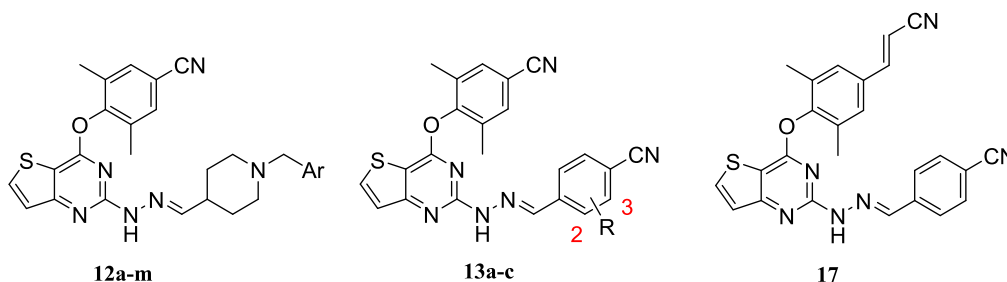
Similarly, treatment of **7** with 3,5-dimethyl-4-hydroxybenzaldehyde yielded **14**, which was reacted with diethyl cyanomethylphosphonate to give intermediate **15** *via* the Wittig-Horner reaction. Then the target compound **17** was obtained *via* hydrazinolysis and nucleophilic addition reaction, successively.

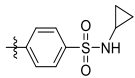
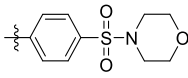
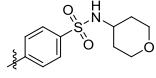
All the novel synthesized compounds were completely characterized by the spectral means including proton nuclear magnetic resonance (¹H NMR), carbon nuclear magnetic resonance (¹³C NMR), and mass spectrometry (MS). The purity of all final compounds was >95% as determined by analytical HPLC.

RESULTS AND DISCUSSION

The target compounds were evaluated for their antiviral potency in MT-4 cell cultures infected with WT HIV-1 strain (IIIB) and double mutant strain K103N+Y181C (RES056). Nevirapine (NVP), etravirine (ETV) and zidovudine (AZT) were selected as reference drugs. The biological evaluation results were interpreted as EC₅₀ (anti-HIV potency), CC₅₀ (cytotoxicity), and SI (selectivity index, CC₅₀/EC₅₀ ratio), which was summarized in **Table 1**.

Table 1. Activity and cytotoxicity against HIV-1 (IIIB and RES056) strains in MT-4 Cells



Compd	R	Ar	EC ₅₀ (μM)		CC ₅₀ (μM)	SI	
			IIIB	RES056		IIIB	RES056
12a	-	4-SO ₂ NH ₂ -Ph	>3.60	-	3.60±0.510	<1	-
12b	-	4-SO ₂ CH ₃ -Ph	>4.62	-	4.62±0.271	<1	-
12c	-	4-CONH ₂ -Ph	>4.65	-	4.65±0.086	<1	-
12d	-	pyridine-4-yl	>5.52	-	5.52±0.340	<1	-
12e	-	4-NO ₂ -Ph	>13.4	-	13.4±11.8	<1	-
12f	-	4-SO ₂ NHCH ₃ -Ph	>3.82	-	3.82±0.329	<1	-
12g	-		>4.03	-	4.03±0.470	<1	-
12h	-	3-CONH ₂ -Ph	>4.68	-	4.68±0.147	<1	-
12i	-	4-CN-Ph	5.85±2.15	>23.6	23.6±6.54	4	<1
12j	-	4-F-Ph	>5.48	-	5.48±2.50	<1	-
12k	-		>14.5	-	14.5±8.43	<1	-
12l	-		>4.42	-	4.42±0.701	<1	-
12m	-	pyridine-2-yl	>4.18	-	4.18±0.951	<1	-
13a	H	-	0.0212±0.005	>58.9	183±0.706	8632	X1
13b	2-F	-	0.0413±0.011	>56.5	182±9.61	4407	X1
13c	3-F	-	0.0257±0.002	>56.5	215±1.37	8366	X1
17	-	-	0.0944±0.055	>96.6	96.6±83.4	1023	<1
NVP	-	-	0.281±0.038	>15.0	>15.0	>53	X1
ETV	-	-	0.004±0.0003	0.035±0.013	2.16±0.107	540	62
AZT	-	-	0.007±0.001	0.017±0.006	>7.48	>1069	>440

^a EC₅₀: concentration of compound required to achieve 50% protection of MT-4 cell cultures against HIV-1-induced cytotoxicity, as determined by the MTT method.

^b CC₅₀: concentration required to reduce the viability of mock-infected cell cultures by 50%, as determined by the MTT method.

^c SI: selectivity index, the ratio of CC₅₀/EC₅₀.

As depicted in the **Table 1**, some of the designed compounds exhibited prominent potency against the WT HIV-1 strain with double-digit nanomolar EC₅₀ values ranging from 21.2 nM to 94.4 nM. Especially, **13a** (EC₅₀ = 0.0212 μM) and **13c** (EC₅₀ = 0.0257 μM) exhibited the most potent activity, being superior to that of NVP (EC₅₀ = 0.281 μM) and comparable to that of AZT (EC₅₀ = 0.007 μM) and ETV (EC₅₀ = 0.004 μM). Besides, **13a** (CC₅₀ = 183 μM, SI = 8632) and **13c** (CC₅₀ = 215 μM, SI = 8366) displayed much lower cytotoxicity and higher selectivity index than ETV (CC₅₀ = 2.16 μM, SI = 540). However, all of the synthesized compounds were inactive to the double mutant strain RES056.

Preliminary structure-activity relationships (SARs) can be concluded from the biological results. First of all, we paid attention to the compounds **12a-m**. We held the view that the newly introduced hydrazone linker could form additional hydrogen bond with Lys103 of the NNIBP. However, almost all the compounds exhibited no activity toward the HIV-1 WT and RES056 at the tested concentration. Only, **12i** demonstrated moderate potency with EC₅₀ value of 5.85 μM. We supposed that the hydrazone linker might change the binding mode of the inhibitor with NNIBP and resulted in the loss of the hydrogen bonding force with Lys103, Lys104 and Val106, indicating that the length of linker have great influence on the antiviral activity.

Furthermore, the replacement of the aminopiperidine with benzene ring resulted in a significantly improved antiviral activity toward WT HIV-1 strains. The activity of **13a** was 10-fold more potent than the reference drug NVP. Introduction of a fluorine atom at the C₂ and C₃ position of the benzonitrile of **13a** yielded **13b** and **13c**, with an EC₅₀ values of 0.0413 and 0.0257 μM respectively, which displayed no obvious advantages over **13a**. In addition, the replacement of the cyano group in the left wing of **13a** with the cyano vinyl group gave compound **17** with slightly reduced activity and increased cytotoxicity (EC₅₀ = 0.0944 μM, CC₅₀ = 96.6 μM).

MOLECULAR MODELING STUDIES

In order to obtain deeper insight into the binding mode of the novel designed compounds in the NNIBP and prove the rationality of our explanation toward the activity, we conducted molecular docking studies of the representative compounds **12a**, **13a**, **13b**, and **13c** with the WT HIV-1 RT crystal structure by utilizing the SurflexeDock SYBYL-X 2.0 software. The co-crystal structure of the reverse transcriptase was selected from the co-crystallization of the small molecule ligand containing aminopiperidine (PDB code: 3M8Q¹⁷) or *p*-cyanoaniline (PDB code: 3MEC¹⁸) on the right wing. Our docking results were visualized by PyMOL. And the docking protocol was illustrated in the computational section.

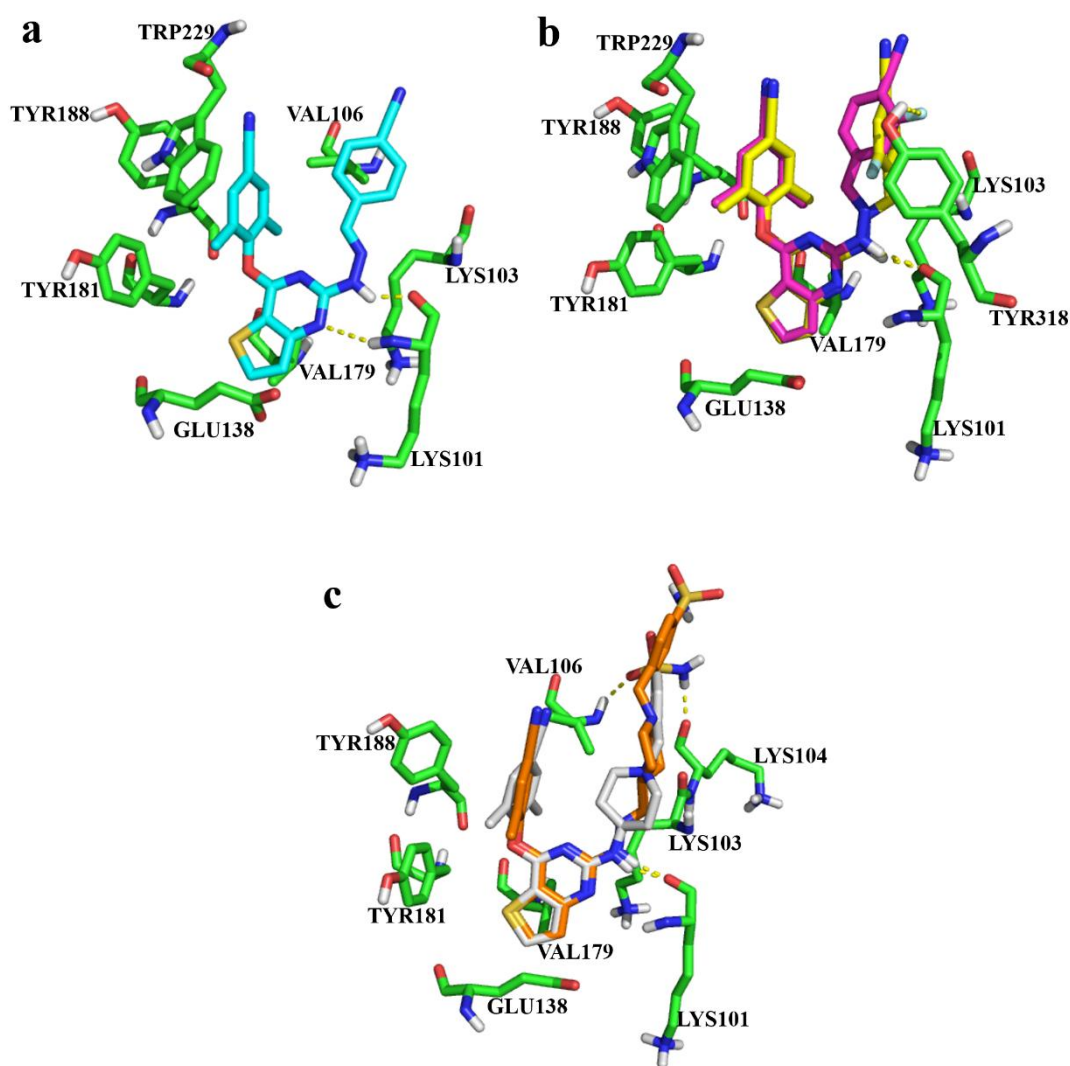


Figure 3. (a) Predicted binding modes of **13a** with the HIV-1 WT RT crystal structure (PDB: 3MEC); (b) Superimposition of **13b** (yellow) and **13c** (magenta) with HIV-1 WT RT (PDB: 3MEC); (c) Superimposition of **12a** (orange) and **6** (white) with HIV-1 WT RT (PDB: 3M8Q). Hydrogen bonds are shown as dashed lines (yellow). Nonpolar hydrogen atoms are hid for clarity.

It is noteworthy that the most potent compound **13a** showed classical horseshoe conformational in the NNIBP similar to other familiar NNRTIs (**Figure 3a**). **13a** has the following characteristic interaction modes: (i) the benzene ring of left wing is stabilized by π - π stacking interactions with aromatic side chains of amino acid residues Tyr181, Tyr188, Phe227 and Trp229; (ii) the thiophene ring points to the NNIBP entrance channel containing Glu138 and Val179 and the sulfur atom forms an electrostatic interaction with Val179. (iii) Remarkably, the *N* atom of the pyrimidine ring and hydrazone linker displays double hydrogen bonding with the main-chain backbone of Lys101, which plays a crucial role in maintaining effective antiviral activity. As shown in **Figure 3b**, the C₃-substituted fluorine atom of **13c** displays direct hydrogen bonding with the conserved amino acid residue Tyr318, which accounts for the more active potency of **13c** than **13b**. However, the hydrogen-bonding interaction between the *N* atom of pyrimidine ring and Lys101 disappeared, which may provide a rational explanation of the slightly reduced activity of **13b** and **13c** compared to **13a**.

Furthermore, we chose the representative compound **12a** to dock into the WT RT binding pocket (**Figure 3c**). Compared with the lead compound **6**, **12a** displays only one hydrogen bonding with Lys103, while **6** forms extensive network of main chain hydrogen bonds with Lys103, Lys104 and Val106. The lack of these main chain hydrogen bonds provides a rational explanation of the inactive potency of **12a-m**.

PHYSICOCHEMICAL PROPERTIES AND MEASURED WATER

SOLUBILITY

Because water solubility and hydrophilicity/lipophilicity are the important factors to evaluate the newly designed compounds, we used free online software (<http://www.molinspiration.com/>) and HPLC to investigate the physicochemical properties and solubility of the potent compounds **13a**, **13b**, **13c** and **17**. As shown in the **Table 2**, the results of physicochemical properties indicated that these four compounds were all conformed well to the Lipinski's rule of five. Furthermore, we also investigated the water solubility and LogP of **13a-c** and **17** by using HPLC. The experimental results demonstrated that **13a-c** have well solubility and favorable LogP value, which can be considered as the promising lead compounds for further optimization.

Table 2. Physicochemical properties and water solubility of **13a**, **13b**, **13c** and **17**

compd	EC ₅₀ (nM)	MW	nON ^a	nOHNH _a	nrotb ^a	TPSA ^a	LogP ^b	pH = 7.0 (μg/mL) ^c	pH = 7.4 (μg/mL) ^d	pH = 2.0 (μg/mL) ^d
Accepted range	-	<500	<10	<5	≤10	<140	<5	-	-	-
13a	21.2	424.11	7	1	5	106.99	1.49	3.91	1.10	5.94
13b	41.3	442.10	7	1	5	106.99	1.53	<<1	3.36	9.36
13c	25.7	442.10	7	1	5	106.99	1.53	0.39	9.76	12.97
17	94.4	450.13	7	1	6	106.99	1.42	<<1	2.08	<<1

^a Using free on-line software (<http://www.molinspiration.com/>); MW = molecular weight; nON = no. of hydrogen bond acceptors; nOHNH = no. of hydrogen bond donors; nrotb = no. of rotatable bonds; TPSA = topological polar surface area.

^b Values were measured at pH 7 by HPLC method in duplicate; LogP = logarithm of partition coefficient.

^c Measured in water at pH 7 by HPLC method in duplicate.

^d Measured in phosphate buffer by HPLC method in duplicate.

CONCLUSION

To sum up, taking our previously reported K-5a2 (compound **6**) as lead compound, a novel series of hydrazone-substituted thiophene [3,2-*d*] pyrimidine derivatives was designed, synthesized and biologically evaluated. Encouragingly, four compounds exhibited remarkable inhibitory activity against WT HIV-1 strain with EC₅₀ values ranging from 21.2 nM to 94.4 nM. Compound **13a** proved to be the most promising inhibitor with low nanomolar EC₅₀ values of 21.2 nM. Moreover, **13a** showed much lower cytotoxicity (CC₅₀ = 183 μM) and higher SI (SI = 8632) than NVP, ETV and AZT. The detailed molecular modeling studies revealed the interactions between the inhibitors and WT HIV-1 RT and rationalized the preliminary SARs. Furthermore, some physicochemical properties were predicted and water solubility were also measured. The current results can provide a useful insight for the development of HIV-1 NNRTIs with improved antiviral activity. Further optimizations of this series of compounds are currently ongoing and will be reported in due course.

EXPERIMENTAL SECTION

Chemistry. All melting points were determined on a micromelting point apparatus and are uncorrected. ¹H NMR and ¹³C NMR spectra were obtained on a Bruker AV-400 spectrometer using DMSO-*d*₆ as the solvent and tetramethylsilane (TMS) as the internal standard. Chemical shifts are given in δ units (ppm) and *J* values were reported in hertz (Hz). Mass spectrometry was recorded on an LC Autosampler device of Standard G1313A instrument. TLC was completed on Silica Gel GF254 for TLC and spots were visualized by irradiation with UV light (λ = 254 nm). Flash column chromatography was performed on columns packed with Silica Gel 60 (200-300 mesh). Solvents were of reagent grade and were purified and dried by standard methods if necessary. Rotary evaporator was used in the concentration of the reaction solutions under reduced pressure. Sample purity was analyzed on a Shimadzu SPD-20A/20AV HPLC system with a Inertsil ODS-SP, 5 μm C18 column (150 mm × 4.6 mm). Purity of all tested compounds was >95%.

*4-((2-chlorothieno[3,2-*d*]pyrimidin-4-yl)oxy)-3,5-dimethylbenzonitrile (8)*. A mixture of 4-hydroxy-3,5-dimethylbenzonitrile (0.79 g, 5.36 mmol) with potassium carbonate (0.81 g, 5.85 mmol) in DMF (15 mL) was reacted in room temperature for 0.5 h; then added 2,4-dichlorothieno[3,2-*d*]pyrimidine (1.0 g, 4.88 mmol) to it. The reaction mixture continued to react for 2 h (monitored by TLC), then the mixture was poured into ice water and left to stand for 1 h. The precipitated white solid was collected by filtration, washed with saturated salt solution, and recrystallized in DMF/H₂O to obtain the desired product **8** as a white solid in 88.3% yield, mp 258-260 °C. ESI-MS: *m/z* 316.3 (*M* + 1). C₁₅H₁₀ClN₃OS (315.02).

*4-((2-hydrazinylthieno[3,2-*d*]pyrimidin-4-yl)oxy)-3,5-dimethylbenzonitrile (9)*. A solution of **8** (1.0 g, 3.17 mmol) in 50 mL of ethanol, and then added 3 mL 80% hydrazine hydrate to it. The mixture was refluxed at 90 °C for 5 h (monitored by TLC). The solution was cooled to room temperature, and 50 mL of ice water was added to it. The resulting precipitate was collected by filtration and dried to give crude product, which was purified by flash column chromatography and recrystallized from ethyl acetate/petroleum ether to afford the intermediate **9** as a white solid in 75.8% yield, mp 219-221 °C. ¹H NMR (400 MHz, DMSO-*d*₆): δ 8.24 (d, *J* = 5.3 Hz, 1H, C₆-thienopyrimidine-H), 8.06 (s, 1H, NH), 7.73 (s, 2H, C₃,C₅-Ph'-H), 7.32 (d, *J* = 5.4 Hz, 1H, C₇-thienopyrimidine-H), 4.09 (s, 2H, NH₂), 2.12 (s, 6H, CH₃×2). ¹³C NMR (100 MHz, DMSO-*d*₆): δ 165.50, 163.60, 162.35, 153.24, 137.00, 133.21, 133.06, 123.70, 119.01, 109.16, 105.90, 16.25. ESI-MS: *m/z* 312.1 (*M* + 1). C₁₅H₁₃N₅OS (311.08).

*(E)-3,5-dimethyl-4-((2-(2-(piperidin-4-ylmethylene)hydrazinyl)thieno[3,2-*d*]pyrimidin-4-yl)oxy)benzonitrile (11)*. A solution of **9** (1.0 g, 3.21 mmol) in 50 mL of ethanol, and then *tert*-butyl 4-formylpiperidine-1-carboxylate (0.82 g, 3.84 mmol) was added to it. The mixture was refluxed at 90 °C for 4 h (monitored by TLC). The solution was cooled to room temperature, and the resulting precipitate was collected by filtration and dried to give crude product **10**, which was used directly in the next step without further purification. Then a solution of **10** (1.0 g, 1.97 mmol) in 5 mL of DCM was added trifluoroacetic acid (TFA) (2.22 mL, 30 mmol) at room temperature, and the solution was stirred for 3 h (monitored by TLC). Then the reaction mixture was alkalized to pH 9 with saturated sodium bicarbonate

solution and washed with 20 mL of saturated salt water. The aqueous phase was extracted with DCM (3×5 mL). The combined organic phase was dried, filtered, and concentrated under vacuum to give **11** as a white solid in 64.5% yield, mp 274–276 °C. ^1H NMR (400 MHz, DMSO- d_6): δ 10.63 (s, 1H, NH), 8.96 (s, 2H), 8.30 (d, $J = 5.3$ Hz, 1H, C₆-thienopyrimidine-H), 7.75 (s, 2H, C₃,C₅-Ph'-H), 7.35 (dd, $J = 33.6, 4.9$ Hz, 2H), 3.31–2.81 (m, 4H), 2.13 (s, 6H, CH₃ $\times 2$), 1.94–1.53 (m, 4H). ^{13}C NMR (100 MHz, DMSO- d_6): δ 165.76, 158.52, 153.26, 147.24, 137.49, 133.27, 133.10, 124.09, 119.00, 109.22, 107.48, 42.80, 36.09, 26.19, 16.28. ESI-MS: m/z 407.3 ($M + 1$). C₂₁H₂₂N₆OS (406.16).

General Procedure for the Preparation of Final Compounds 12a-m. Compound **11** was dissolved in 5 mL of anhydrous DMF, followed by addition of the anhydrous K₂CO₃ (1.2 equiv) and appropriate substituted benzyl chloride (bromide) or picolyl chloride hydrochloride (1.1 equiv). The reaction mixture was stirred at room temperature for 6 h (monitored by TLC). The solvent was removed under vacuum and the residue was taken up in 20 mL of water and extracted with ethyl acetate (3×10 mL). Then the organic phase was washed with saturated sodium chloride (2×10 mL), dried, filtered, and purified by flash column chromatography. Recrystallized from ethyl acetate/petroleum ether to afford the target compounds **12a-m**.

(*E*)-4-((4-((2-(4-(4-cyano-2,6-dimethylphenoxy)thieno[3,2-*d*]pyrimidin-2-yl)hydrazono)methyl)piperidin-1-yl)methyl)benzenesulfonamide (**12a**). Recrystallized from ethyl acetate/petroleum ether as a white solid, 53.1% yield, mp 193–195 °C. ^1H NMR (400 MHz, DMSO- d_6): δ 10.44 (s, 1H, NH), 8.21 (d, $J = 5.4$ Hz, 1H, N=CH), 7.80–7.60 (m, 4H), 7.42 (d, $J = 8.0$ Hz, 2H, C₃,C₅-Ph"-H), 7.31 (d, $J = 5.4$ Hz, 1H, C₆-thienopyrimidine-H), 7.24 (d, $J = 9.0$ Hz, 3H), 3.45 (s, 2H, N-CH₂), 2.70 (d, $J = 11.5$ Hz, 2H), 2.06 (s, 7H), 2.00–1.88 (m, 2H), 1.65–1.53 (m, 2H), 1.42–1.29 (m, 2H). ^{13}C NMR (100 MHz, DMSO- d_6): δ 165.81, 162.52, 158.56, 153.27, 149.35, 143.36, 143.11, 137.36, 133.28, 133.09, 129.41, 126.05, 124.07, 109.23, 107.28, 62.15, 52.98, 38.72, 29.90, 16.27. ESI-MS: m/z 576.3 ($M + 1$). C₂₈H₂₉N₇O₃S₂ (575.18). HPLC purity: 96.67%.

(E)-3,5-dimethyl-4-((2-(2-((1-(4-(methylsulfonyl)benzyl)piperidin-4-yl)methylene)hydrazinyl)thieno[3,2-d]pyrimidin-4-yl)oxy)benzonitrile (**12b**). Recrystallized from ethyl acetate/petroleum ether as a white solid, 61.2% yield, mp 216-218 °C. ¹H NMR (400 MHz, DMSO-*d*₆): δ 10.45 (s, 1H, NH), 8.21 (d, *J* = 5.4 Hz, 1H, N=CH), 7.81 (d, *J* = 8.0 Hz, 2H, C₃,C₅-Ph"-H), 7.66 (s, 2H, C₃,C₅-Ph'-H), 7.51 (d, *J* = 8.1 Hz, 2H, C₂,C₆-Ph"-H), 7.31 (d, *J* = 5.4 Hz, 1H, C₆-thienopyrimidine-H), 7.24 (d, *J* = 5.3 Hz, 1H, C₇-thienopyrimidine-H), 3.49 (s, 2H, N-CH₂), 3.14 (s, 3H, SO₂CH₃), 2.70 (d, *J* = 11.5 Hz, 2H), 2.24–1.84 (m, 9H), 1.60 (dd, *J* = 13.5, 3.8 Hz, 2H), 1.47–1.27 (m, 2H). ¹³C NMR (100 MHz, DMSO-*d*₆): δ 158.58, 153.27, 149.26, 145.53, 139.76, 137.36, 133.28, 133.08, 129.73, 127.39, 124.07, 118.97, 109.21, 62.09, 53.03, 44.07, 38.68, 29.88, 16.28. ESI-MS: *m/z* 575.5 (*M* + 1). C₂₉H₃₀N₆O₃S₂ (574.18). HPLC purity: 99.15%.

(E)-4-((4-((2-(4-(4-cyano-2,6-dimethylphenoxy)thieno[3,2-d]pyrimidin-2-yl)hydrazono)methyl)piperidin-1-yl)methyl)benzamide (**12c**). Recrystallized from ethyl acetate/petroleum ether as a white solid, 54.5% yield, mp 247-249 °C. ¹H NMR (400 MHz, DMSO-*d*₆): δ 10.51 (s, 1H, NH), 8.28 (d, *J* = 5.3 Hz, 1H, N=CH), 7.93 (s, 1H), 7.83 (d, *J* = 7.9 Hz, 2H, C₃,C₅-Ph"-H), 7.74 (s, 2H, CONH₂), 7.46–7.21 (m, 5H), 3.50 (s, 2H, N-CH₂), 2.77 (d, *J* = 11.3 Hz, 2H), 2.13 (s, 7H), 2.06–1.94 (m, 2H), 1.66 (dd, *J* = 13.2, 3.8 Hz, 2H), 1.51–1.34 (m, 2H). ¹³C NMR (100 MHz, DMSO-*d*₆): δ 168.24, 165.81, 162.52, 158.57, 153.27, 149.37, 142.51, 137.34, 133.37, 133.28, 133.08, 128.83, 127.87, 124.07, 109.23, 62.42, 53.00, 38.77, 29.91, 16.27. ESI-MS: *m/z* 540.6 (*M* + 1). C₂₉H₂₉N₇O₂S (539.21). HPLC purity: 98.71%.

(E)-3,5-dimethyl-4-((2-(2-((1-(pyridin-4-ylmethyl)piperidin-4-yl)methylene)hydrazinyl)thieno[3,2-d]pyrimidin-4-yl)oxy)benzonitrile (**12d**). Recrystallized from ethyl acetate/petroleum ether as a white solid, 43.8% yield, mp 214-216 °C. ¹H NMR (400 MHz, DMSO-*d*₆): δ 10.53 (s, 1H, NH), 8.58–8.44 (m, 2H), 8.29 (d, *J* = 5.3 Hz, 1H, C₆-thienopyrimidine-H), 7.74 (s, 2H, C₃,C₅-Ph'-H), 7.38 (d, *J* = 5.4 Hz, 1H, C₇-thienopyrimidine-H), 7.35–7.28 (m, 3H), 3.49 (s, 2H, N-CH₂), 2.77 (d, *J* = 11.4 Hz, 2H), 2.13 (s, 8H), 1.67 (dd, *J* = 13.5, 3.8 Hz, 2H), 1.54–1.30 (m, 3H). ¹³C NMR (100 MHz, DMSO-*d*₆): δ 165.80, 162.52, 158.57, 153.27, 149.96, 149.25, 148.28, 137.36, 133.28,

133.08, 124.08, 118.98, 109.22, 61.43, 53.04, 38.64, 29.85, 16.28. ESI-MS: m/z 499.4 ($M + 1$). $C_{27}H_{27}N_7OS$ (497.20). HPLC purity: 99.91%.

(*E*)-3,5-dimethyl-4-((2-(2-((1-(4-nitrobenzyl)piperidin-4-yl)methylene)hydrazinyl)thieno[3,2-*d*]pyrimidin-4-yl)oxy)benzonitrile (**12e**). Recrystallized from ethyl acetate/petroleum ether as a white solid, 46.9% yield, mp 220-222 °C. 1H NMR (400 MHz, DMSO- d_6): δ 10.53 (s, 1H, NH), 8.28 (d, $J = 5.3$ Hz, 1H, N=CH), 8.24–8.14 (m, 2H, C_3, C_5 -Ph"-H), 7.73 (s, 2H, C_3, C_5 -Ph'-H), 7.59 (d, $J = 8.4$ Hz, 2H, C_2, C_6 -Ph"-H), 7.38 (d, $J = 5.4$ Hz, 1H, C_6 -thienopyrimidine-H), 7.31 (d, $J = 5.3$ Hz, 1H, C_7 -thienopyrimidine-H), 3.59 (s, 2H, N-CH₂), 2.77 (dt, $J = 11.4, 3.4$ Hz, 2H), 2.30–1.90 (m, 9H), 1.67 (dd, $J = 13.1, 3.8$ Hz, 2H), 1.53–1.33 (m, 2H). ^{13}C NMR (100 MHz, DMSO- d_6): δ 165.80, 162.52, 158.58, 153.27, 149.22, 147.65, 146.94, 137.37, 133.27, 133.08, 129.99, 124.07, 123.82, 118.97, 109.21, 61.83, 53.02, 38.63, 29.87, 16.28. ESI-MS: m/z 542.5 ($M + 1$). $C_{28}H_{27}N_7O_3S$ (541.19). HPLC purity: 98.91%.

(*E*)-4-((4-((2-(4-(4-cyano-2,6-dimethylphenoxy)thieno[3,2-*d*]pyrimidin-2-yl)hydrazono)methyl)piperidin-1-yl)methyl)-*N*-methylbenzenesulfonamide (**12f**). Recrystallized from ethyl acetate/petroleum ether as a white solid, 56.5% yield, mp 143-145 °C. 1H NMR (400 MHz, DMSO- d_6): δ 10.44 (s, 1H, NH), 8.21 (d, $J = 5.3$ Hz, 1H, N=CH), 7.66 (t, $J = 4.1$ Hz, 4H), 7.46 (d, $J = 8.0$ Hz, 2H, C_2, C_6 -Ph"-H), 7.32 (dd, $J = 11.7, 5.2$ Hz, 2H), 7.24 (d, $J = 5.4$ Hz, 1H, C_7 -thienopyrimidine-H), 3.47 (s, 2H, N-CH₂), 2.80–2.62 (m, 2H), 2.34 (d, $J = 5.0$ Hz, 3H, NHCH₃), 2.06 (s, 7H), 1.95 (t, $J = 11.1$ Hz, 2H), 1.60 (dd, $J = 13.2, 3.8$ Hz, 2H), 1.45–1.27 (m, 2H). ^{13}C NMR (100 MHz, DMSO- d_6): δ 165.81, 158.58, 153.27, 149.30, 144.13, 138.15, 137.35, 133.28, 133.08, 129.61, 127.11, 124.07, 118.97, 109.23, 62.13, 53.02, 38.69, 29.88, 29.15, 16.27. ESI-MS: m/z 590.5 ($M + 1$). $C_{29}H_{31}N_7O_3S_2$ (589.19). HPLC purity: 98.95%.

(*E*)-4-((4-((2-(4-(4-cyano-2,6-dimethylphenoxy)thieno[3,2-*d*]pyrimidin-2-yl)hydrazono)methyl)piperidin-1-yl)methyl)-*N*-cyclopropylbenzenesulfonamide (**12g**). Recrystallized from ethyl acetate/petroleum ether as a white solid, 50.8% yield, mp 129-131 °C. 1H NMR (400 MHz, DMSO- d_6): δ 10.44 (s, 1H, NH), 8.21 (d, $J = 5.3$ Hz, 1H, N=CH), 7.80 (d, $J = 2.6$ Hz,

1H, SO₂NH), 7.75–7.60 (m, 4H), 7.46 (d, *J* = 8.0 Hz, 2H, C₂,C₆-Ph"-H), 7.31 (d, *J* = 5.3 Hz, 1H, C₆-thienopyrimidine-H), 7.24 (d, *J* = 5.4 Hz, 1H, C₇-thienopyrimidine-H), 3.48 (s, 2H, N-CH₂), 2.86–2.61 (m, 2H), 2.26–1.85 (m, 10H), 1.60 (dd, *J* = 12.9, 3.9 Hz, 2H), 1.46–1.25 (m, 2H), 0.51–0.23 (m, 4H, CH₂CH₂). ¹³C NMR (100 MHz, DMSO-*d*₆): δ 165.81, 153.27, 149.30, 144.15, 139.15, 137.35, 133.28, 133.08, 129.56, 127.23, 124.07, 118.97, 109.22, 62.13, 53.00, 38.70, 29.88, 24.56, 16.27, 5.59. ESI-MS: *m/z* 616.5 (*M* + 1). C₃₁H₃₃N₇O₃S₂ (615.21). HPLC purity: 98.57%.

(*E*)-3-((4-((2-(4-(4-cyano-2,6-dimethylphenoxy)thieno[3,2-*d*]pyrimidin-2-yl)hydrazono)methyl)piperidin-1-yl)methyl)benzamide (**12h**). Recrystallized from ethyl acetate/petroleum ether as a white solid, 51.6% yield, mp 136–138 °C. ¹H NMR (400 MHz, DMSO-*d*₆): δ 10.44 (s, 1H, NH), 8.21 (d, *J* = 5.3 Hz, 1H, N=CH), 7.91 (s, 1H), 7.83–7.59 (m, 4H), 7.46–7.17 (m, 5H), 3.43 (s, 2H, N-CH₂), 2.87–2.63 (m, 2H), 2.06 (s, 8H), 1.69–1.51 (m, 2H), 1.34 (d, *J* = 18.4 Hz, 3H). ¹³C NMR (100 MHz, DMSO-*d*₆): δ 168.41, 165.81, 162.52, 158.57, 153.27, 149.37, 137.33, 134.66, 133.27, 133.08, 132.07, 128.48, 126.47, 124.08, 118.97, 109.22, 107.27, 62.64, 52.94, 38.78, 29.85, 16.27. ESI-MS: *m/z* 540.2 (*M* + 1). C₂₉H₂₉N₇O₂S (539.21). HPLC purity: 97.02%.

(*E*)-4-((2-(2-((1-(4-cyanobenzyl)piperidin-4-yl)methylene)hydrazinyl)thieno[3,2-*d*]pyrimidin-4-yl)oxy)-3,5-dimethylbenzonitrile (**12i**). Recrystallized from ethyl acetate/petroleum ether as a white solid, 46.2% yield, mp 248–250 °C. ¹H NMR (400 MHz, DMSO-*d*₆): δ 10.52 (s, 1H, NH), 8.29 (d, *J* = 5.4 Hz, 1H, N=CH), 7.80 (d, *J* = 8.0 Hz, 2H, C₃,C₅-Ph"-H), 7.74 (s, 2H, C₃,C₅-Ph'-H), 7.52 (d, *J* = 7.9 Hz, 2H, C₂,C₆-Ph"-H), 7.38 (d, *J* = 5.4 Hz, 1H, C₆-thienopyrimidine-H), 7.31 (d, *J* = 5.3 Hz, 1H, C₇-thienopyrimidine-H), 3.55 (s, 2H, N-CH₂), 2.89 (s, 1H), 2.75 (d, *J* = 15.5 Hz, 3H), 2.13 (s, 6H, CH₃×2), 1.74–1.57 (m, 2H), 1.55–1.28 (m, 3H). ¹³C NMR (100 MHz, DMSO-*d*₆): δ 165.80, 162.52, 158.57, 153.27, 137.37, 133.28, 133.11, 133.08, 132.61, 130.18, 129.88, 124.07, 119.42, 118.98, 109.21, 107.26, 52.98, 29.86, 16.28. ESI-MS: *m/z* 522.4 (*M* + 1). C₂₉H₂₇N₇OS (521.20). HPLC purity: 97.07%.

(E)-4-((2-(2-((1-(4-fluorobenzyl)piperidin-4-yl)methylene)hydrazinyl)thieno[3,2-*d*]pyrimidin-4-yl)oxy)-3,5-dimethylbenzonitrile (**12j**). Recrystallized from ethyl acetate/petroleum ether as a white solid, 58.7% yield, mp 227-229 °C. ¹H NMR (400 MHz, DMSO-*d*₆): δ 10.50 (s, 1H, NH), 8.28 (d, *J* = 5.4 Hz, 1H, N=CH), 7.73 (s, 2H, C₃,C₅-Ph'-H), 7.44–7.24 (m, 4H), 7.13 (t, *J* = 8.7 Hz, 2H), 3.43 (s, 2H, N-CH₂), 2.81–2.71 (m, 2H), 2.12 (s, 6H, CH₃×2), 1.98 (d, *J* = 6.9 Hz, 3H), 1.71–1.59 (m, 2H), 1.47–1.32 (m, 2H). ¹³C NMR (100 MHz, DMSO-*d*₆): δ 165.81, 162.52, 158.58, 153.27, 149.35, 137.35, 133.28, 133.08, 130.99, 130.91, 124.07, 118.97, 115.40, 115.19, 109.22, 107.26, 61.91, 52.85, 38.80, 29.89, 16.27, 14.56. ESI-MS: *m/z* 515.4 (*M* + 1). C₂₈H₂₇FN₆OS (514.20). HPLC purity: 95.19%.

(E)-3,5-dimethyl-4-((2-(2-((1-(4-(morpholinosulfonyl)benzyl)piperidin-4-yl)methylene)hydrazinyl)thieno[3,2-*d*]pyrimidin-4-yl)oxy)benzonitrile (**12k**). Recrystallized from ethyl acetate/petroleum ether as a white solid, 63.1% yield, mp 139-141 °C. ¹H NMR (400 MHz, DMSO-*d*₆): δ 10.45 (s, 1H, NH), 8.21 (d, *J* = 5.3 Hz, 1H, N=CH), 7.64 (d, *J* = 18.2 Hz, 4H), 7.53 (d, *J* = 8.0 Hz, 2H, C₂,C₆-Ph"-H), 7.31 (d, *J* = 5.4 Hz, 1H, C₆-thienopyrimidine-H), 7.25 (d, *J* = 5.3 Hz, 1H, C₇-thienopyrimidine-H), 3.71–3.40 (m, 6H), 2.91–2.63 (m, 7H), 2.06 (s, 8H), 1.60 (d, *J* = 11.2 Hz, 2H), 1.49–1.21 (m, 2H). ¹³C NMR (100 MHz, DMSO-*d*₆): δ 165.81, 158.58, 153.27, 137.36, 133.28, 133.07, 129.76, 128.15, 124.06, 109.22, 65.72, 62.06, 53.04, 46.37, 38.68, 29.86, 16.27. ESI-MS: *m/z* 646.3 (*M* + 1). C₃₂H₃₅N₇O₄S₂ (645.22). HPLC purity: 96.91%.

(E)-4-((4-((2-(4-(4-cyano-2,6-dimethylphenoxy)thieno[3,2-*d*]pyrimidin-2-yl)hydrazono)methyl)piperidin-1-yl)methyl)-*N*-(tetrahydro-2*H*-pyran-4-yl)benzenesulfonamide (**12l**). Recrystallized from ethyl acetate/petroleum ether as a white solid, 56.2% yield, mp 140-142 °C. ¹H NMR (400 MHz, DMSO-*d*₆): δ 10.44 (s, 1H, NH), 8.21 (d, *J* = 5.4 Hz, 1H, N=CH), 7.80–7.60 (m, 5H), 7.43 (d, *J* = 8.0 Hz, 2H, C₂,C₆-Ph"-H), 7.31 (d, *J* = 5.4 Hz, 1H, C₆-thienopyrimidine-H), 7.24 (d, *J* = 5.4 Hz, 1H, C₇-thienopyrimidine-H), 3.75–3.56 (m, 2H), 3.47 (s, 2H), 3.14 (td, *J* = 11.4, 2.4 Hz, 3H), 2.70 (d, *J* = 10.9 Hz, 2H), 2.06 (s, 6H, CH₃×2), 1.95 (t, *J* = 11.0 Hz, 2H), 1.68–1.53 (m, 2H), 1.50–1.17 (m, 7H). ¹³C NMR (100 MHz, DMSO-*d*₆): δ 165.81, 162.52, 158.58, 153.27, 149.31, 143.92, 141.00, 137.35, 133.28,

133.08, 129.60, 126.71, 124.07, 109.22, 65.97, 62.09, 53.01, 49.68, 39.65, 38.70, 33.75, 29.88, 16.27. ESI-MS: m/z 661.3 ($M + 1$). $C_{33}H_{37}N_7O_4S_2$ (659.23). HPLC purity: 99.79%.

(*E*)-3,5-dimethyl-4-((2-(2-((1-(pyridin-2-ylmethyl)piperidin-4-yl)methylene)hydrazinyl)thieno[3,2-*d*]pyrimidin-4-yl)oxy)benzonitrile (**12m**). Recrystallized from ethyl acetate/petroleum ether as a white solid, 49.5% yield, mp 116–118 °C. 1H NMR (400 MHz, DMSO- d_6): δ 10.45 (s, 1H, NH), 8.41 (dd, $J = 5.0, 1.7$ Hz, 1H), 8.21 (d, $J = 5.4$ Hz, 1H, N=CH), 7.78–7.54 (m, 3H), 7.37 (d, $J = 7.8$ Hz, 1H), 7.31 (d, $J = 5.3$ Hz, 1H, C₆-thienopyrimidine-H), 7.24 (d, $J = 5.4$ Hz, 1H, C₇-thienopyrimidine-H), 7.21–7.14 (m, 1H), 3.51 (s, 2H), 2.74 (d, $J = 11.2$ Hz, 2H), 2.06 (s, 9H), 1.60 (dd, $J = 13.4, 3.8$ Hz, 2H), 1.46–1.20 (m, 2H). ^{13}C NMR (100 MHz, DMSO- d_6): δ 165.81, 158.58, 153.27, 149.31, 149.18, 137.35, 136.92, 133.28, 133.07, 124.07, 123.01, 122.52, 118.97, 109.22, 64.59, 53.17, 38.65, 29.90, 16.27. ESI-MS: m/z 498.6 ($M + 1$). $C_{27}H_{27}N_7OS$ (497.20). HPLC purity: 95.10%.

4-((2-chlorothiopheno[3,2-*d*]pyrimidin-4-yl)oxy)-3,5-dimethylbenzaldehyde (**14**). A mixture of 4-hydroxy-3,5-dimethylbenzaldehyde (0.88 g, 5.85 mmol) and potassium carbonate (1.35 g, 9.75 mmol) in 15 mL of DMF was stirred at 25 °C for 15 min, and then added 2,4-dichlorothiopheno[3,2-*d*]pyrimidine (1.0 g, 4.88 mmol) to it. The mixture was stirred for another 1.5 h (monitored by TLC), then poured into 30 mL of ice water and left to stand for 1 h. The precipitated white solid was collected by filtration, washed with cold water, and recrystallized from DMF/H₂O to provide **14** as a white solid in 91.3% yield, mp 285–287 °C. ESI-MS: m/z 319.1 ($M + 1$). $C_{15}H_{11}ClN_2O_2S$ (318.02).

(*E*)-3-(4-((2-chlorothiopheno[3,2-*d*]pyrimidin-4-yl)oxy)-3,5-dimethylphenyl)acrylonitrile (**15**). A mixture of (EtO)₂P(O)CH₂CN (0.67 g, 3.76 mmol) and *t*-BuOK (0.71 g, 6.27 mmol) in 10 mL of THF was stirred for 1 h at 0 °C, and then a solution of **14** (1.0 g, 3.14 mmol) in 10 mL of THF was slowly added to it. The mixture was stirred for another 1 h (monitored by TLC). The mixture was poured into 20 mL of ice water, and the precipitate was collected, washed with cold water, and dried to afford **15** as a white solid in 85.7% yield, mp 225–227 °C. ESI-MS: m/z 342.0 ($M + 1$). $C_{17}H_{12}ClN_3OS$ (341.04).

(E)-3-(4-((2-hydrazinylthieno[3,2-*d*]pyrimidin-4-yl)oxy)-3,5-dimethylphenyl)acrylonitrile (**16**). The synthetic method was similar to that of **9** and starting with material **15** (0.34g, 1.0 mmol). White solid, 81.6% yield, mp 193-195 °C. ESI-MS: *m/z* 338.4 (*M* + 1). C₁₇H₁₅N₅OS (337.10).

General Procedure for the Preparation of Final Compounds 13a-c and 17. Compounds **9** or **16** were added to anhydrous ethanol (10 mL), followed by addition of appropriate substituted or not substituted 4-cyanobenzaldehyde (1.1 equiv). The reaction mixture was refluxed at 90 °C for 4 h (monitored by TLC). The solvent was removed under vacuum and recrystallized from ethanol to afford the target compounds **13a-c** and **17**.

(E)-4-((2-(2-(4-cyanobenzylidene)hydrazinyl)thieno[3,2-*d*]pyrimidin-4-yl)oxy)-3,5-dimethylbenzonitrile (**13a**). Recrystallized from ethanol as a white solid, 70.4% yield, mp 280-282 °C. ¹H NMR (400 MHz, DMSO-*d*₆): δ 11.42 (s, 1H, NH), 8.37 (d, *J* = 5.3 Hz, 1H, C₆-thienopyrimidine-H), 8.10 (s, 1H, N=CH), 7.85 (d, *J* = 8.2 Hz, 2H, C₂,C₆-Ph"-H), 7.79 (s, 2H, C₃,C₅-Ph'-H), 7.75 (d, *J* = 8.1 Hz, 2H, C₃,C₅-Ph"-H), 7.50 (d, *J* = 5.3 Hz, 1H, C₇-thienopyrimidine-H), 2.17 (s, 6H, CH₃×2). ¹³C NMR (100 MHz, DMSO-*d*₆): δ 165.67, 162.70, 158.11, 153.27, 140.25, 139.75, 137.93, 133.34, 133.12, 133.04, 127.16, 124.22, 119.33, 119.01, 110.98, 109.32, 108.58, 16.32. ESI-MS: *m/z* 425.4 (*M* + 1). C₂₃H₁₆N₆OS (424.11). HPLC purity: 99.75%.

(E)-4-((2-(2-(4-cyano-2-fluorobenzylidene)hydrazinyl)thieno[3,2-*d*]pyrimidin-4-yl)oxy)-3,5-dimethylbenzonitrile (**13b**). Recrystallized from ethanol as a white solid, 74.5% yield, mp 265-267 °C. ¹H NMR (400 MHz, DMSO-*d*₆): δ 11.56 (s, 1H, NH), 8.39 (d, *J* = 5.4 Hz, 1H, C₆-thienopyrimidine-H), 8.26 (s, 1H, N=CH), 8.08-7.85 (m, 2H), 7.79 (s, 2H, C₃,C₅-Ph'-H), 7.71 (dd, *J* = 8.1, 1.5 Hz, 1H), 7.51 (d, *J* = 5.4 Hz, 1H, C₇-thienopyrimidine-H), 2.16 (s, 6H, CH₃×2). ¹³C NMR (100 MHz, DMSO-*d*₆): δ 165.62, 162.74, 157.89, 153.24, 138.07, 133.33, 133.13, 132.35, 129.13, 128.54, 128.44, 126.95, 124.24, 120.68, 120.43, 118.99, 118.22, 112.09, 109.36, 108.90, 16.30. ESI-MS: *m/z* 443.5 (*M* + 1). C₂₃H₁₅FN₆OS (442.10). HPLC purity: 99.69%.

(E)-4-((2-(2-(4-cyano-3-fluorobenzylidene)hydrazinyl)thieno[3,2-*d*]pyrimidin-4-yl)oxy)-3,5-dimethylbenzonitrile (**13c**). Recrystallized from ethanol as a white solid, 71.2% yield, mp 286-288 °C. ¹H NMR (400 MHz, DMSO-*d*₆): δ 11.59 (s, 1H, NH), 8.39 (d, *J* = 5.3 Hz, 1H, C₆-thienopyrimidine-H), 8.07 (s, 1H, N=CH), 7.92 (t, *J* = 7.4 Hz, 1H), 7.79 (s, 2H, C₃,C₅-Ph'-H), 7.58 (d, *J* = 8.7 Hz, 2H, C₂,C₆-Ph''-H), 7.50 (d, *J* = 5.3 Hz, 1H, C₇-thienopyrimidine-H), 2.16 (s, 6H, CH₃×2). ¹³C NMR (100 MHz, DMSO-*d*₆): δ 165.59, 162.74, 157.99, 153.24, 143.60, 143.52, 138.26, 138.06, 134.64, 133.34, 133.07, 124.20, 123.38, 123.35, 118.94, 114.65, 113.21, 113.01, 109.37, 108.84, 99.46, 39.65, 16.32. ESI-MS: *m/z* 443.5 (*M* + 1). C₂₃H₁₅FN₆OS (442.10). HPLC purity: 99.92%.

4-((*E*)-(2-(4-(4-((*E*)-2-cyanovinyl)-2,6-dimethylphenoxy)thieno[3,2-*d*]pyrimidin-2-yl)hydrazono)methyl)benzonitrile (**17**). Recrystallized from ethanol as a white solid, 67.3% yield, mp 262-264 °C. ¹H NMR (400 MHz, DMSO-*d*₆): δ 11.41 (s, 1H, NH), 8.34 (d, *J* = 5.4 Hz, 1H, C₆-thienopyrimidine-H), 8.12 (s, 1H, N=CH), 7.84 (d, *J* = 8.2 Hz, 2H, C₂,C₆-Ph''-H), 7.75 (d, *J* = 8.2 Hz, 2H, C₃,C₅-Ph'-H), 7.66 (d, *J* = 16.8 Hz, 1H, ArCH=), 7.54 (s, 2H, C₃,C₅-Ph'-H), 7.49 (d, *J* = 5.4 Hz, 1H, C₇-thienopyrimidine-H), 6.48 (d, *J* = 16.7 Hz, 1H, =CHCN), 2.14 (s, 6H, CH₃×2). ¹³C NMR (100 MHz, DMSO-*d*₆): δ 165.52, 163.10, 158.21, 151.57, 150.37, 140.28, 139.72, 137.73, 133.06, 132.18, 131.95, 128.71, 127.16, 124.20, 119.34, 110.96, 108.69, 97.12, 16.58. ESI-MS: *m/z* 451.4 (*M* + 1). C₂₅H₁₈N₆OS (450.13). HPLC purity: 99.89%.

In Vitro Anti-HIV Assay. Antiviral activity and cytotoxicity of the synthesized compounds were evaluated against WT HIV-1 strain (IIIB) and double RT mutant strain (K103N+Y181C) in MT-4 cell cultures utilizing the 3-(4,5-dimethylthiazol-2-yl)-2,5-diphenyltetrazolium bromide (MTT) method as described previously.^{19,20} Stock solutions (10× final concentration) of test compounds were added in 25 μL volumes to two series of triplicate wells in order to allow simultaneous evaluation of the effects on mock- and HIV-infected cells. Using a Biomek 3000 robot (Beckman Instruments, Fullerton, CA) to dilute the test compounds to 5-fold serially (final 200 μL volume per well) in flat-bottomed 96-well microtiter trays, including untreated control HIV-1 and mock-infected cell samples for each sample. HIV-1 (IIIB) and double mutant HIV-1 strain

(K103N+Y181C) stock (50 μ L at 100-300 CCID₅₀) (50% cell culture infectious dose) or culture medium was added to either the infected or mock-infected wells of the microtiter tray. Mock-infected cells were used to evaluate the effect of test compounds on uninfected cells in order to assess the cytotoxicity of compounds. Exponentially growing MT-4 cells were centrifuged for 5 min at 1000 rpm and the supernatant was discarded. The MT-4 cells were resuspended at 6×10^5 cells/mL, and 50 μ L volumes were transferred to the microtiter tray wells. After 5 days of infection, the viability of mock- and HIV-infected cells was examined spectrophotometrically by using the MTT method. The 50% cytotoxic concentration (CC₅₀) was defined as the concentration of compound that reduced the absorbance (OD₅₄₀) of mock-infected MT-4 cells by 50%. The 50% effective concentration (EC₅₀) was defined as the concentration of compound that achieved 50% protection from the cytopathic effect of the virus in infected cells.

Molecular Simulations. Molecular simulations was performed with the Tripos molecular modeling package Sybyl-X 2.0. All the molecules for docking were built using standard bond lengths and angles from Sybyl-X 2.0/Base Builder. The molecules (**12a**, **13a**, **13b**, **13c** and **6**) were optimized by using the Tripos force field for 1000 generations two times or more until the minimized conformers of the ligand were the same. The protein was prepared by removing the water molecules and ligand and adding polar hydrogen atoms. The published crystal structures of the liganded HIV-1 RT complex (PDB codes: 3MEC and 3M8Q) were retrieved from the Protein Data Bank. The flexible docking method (Surflex-Dock) docks the ligand automatically into the ligand-binding site of the receptor by using a protocol-based approach and an empirically-derived scoring function. The protocol is a computational representation of a putative ligand that binds to the intended binding site and is a unique and essential element of the docking algorithm. The scoring function in Surflex-Dock, containing hydrophobic, polar, repulsive, entropic, and solvation terms, was trained to estimate the dissociation constant (K_d) expressed in $-\log(K_d)^2$. Surflex-Dock default settings were used for other parameters, such as the maximum number of rotatable bonds per molecule (set to 100) and the maximum number of poses per ligand (set to 20). During the docking procedure, all of the single bonds in residue side-chains inside the

defined RT binding pocket were regarded as rotatable or flexible, and the ligand was allowed to rotate at all single bonds and move flexibly within the tentative binding pocket. The atomic charges were recalculated using the Kollman all-atom approach for the protein and the Gasteiger-Hückel approach for the ligand. The binding interaction energy was calculated, including van der Waals, electrostatic, and torsional energy terms defined in the Tripos force field. The structure optimization was performed for 10,000 generations using a genetic algorithm, and the 20-best-scoring ligand-protein complexes were kept for further analysis. The $-\log(K_d)^2$ values of the 20-best-scoring complexes, representing the binding affinities of ligand with RT, encompassed a wide range of functional classes (10^{-2} - 10^{-9}). Hence, only the highest-scoring 3D structural model of ligand-bound RT was chosen to define the binding interaction.

Measurements of water solubility and LogP. Water solubility was measured in water at pH 7.0 and phosphate buffer at pH 7.4 and 2.0 by using an HPLC-UV method.²¹ Compounds were initially dissolved in DMSO at 10 mg/mL. 10 μ L of this stock solution was spiked into purified water (1 mL) with the final DMSO concentration being 1%. The mixture was ultrasonic for 2 h at room temperature and restored at room temperature overnight. The saturated solution was filtrated through a filter membrane (pore size = 0.22 μ m) and transferred to other Eppendorf tubes for analysis by HPLC-UV. The sample was performed in duplicate. For quantification, a model LC-20AT HPLC-UV (SHIMADZU) system was used with an Inertsil[®] ODS-SP-C18 column (150 mm \times 4.6 mm, 5 μ m) and MeOH/water as eluant. The flow rate was 1.0 mL/min, and injection volume was 20 μ L. Aqueous concentration was determined by comparison of the peak area of the saturated solution with a standard curve plotted peak area versus known concentrations, which were prepared by solutions in MeOH at 200, 100, 50, 25, and 12.5 μ g/mL.

DMSO stock solution 1 mg/mL was prepared, and then 20 μ L of this solution was added into *n*-octanol (1 mL) and H₂O (1 mL). The mixture was ultrasonic for 2 h at room temperature and left to sit overnight. Each solution (~0.4 mL) was transferred from two phases, respectively, into other eppendorf tubes for HPLC analysis. The instrument and

conditions were the same as those for solubility determination. The P (partition coefficient) value was calculated by the peak area ratios in *n*-octanol and in H₂O.

AUTHOR INFORMATION

Corresponding Authors

*P.Z.: e-mail, zhanpeng1982@sdu.edu.cn; phone, 086-531-88382005.

*X.L.: e-mail, xinyongl@sdu.edu.cn; phone, 086-531-88380270.

Funding

Financial support from the National Natural Science Foundation of China (NSFC Grants 81273354, 81573347), Key Project of NSFC for International Cooperation (Grant 81420108027), Young Scholars Program of Shandong University (YSPSDU Grant 2016WLJH32), the Fundamental Research Funds of Shandong University (Grant 2017JC006), Key Research and Development Project of Shandong Province (Grant 2017CXGC1401), and KU Leuven (Grant GOA 10/014) is gratefully acknowledged.

Notes

The authors declare no competing financial interest.

ACKNOWLEDGMENTS

We thank K. Erven, K. Uyttersprot, and C. Heens for technical assistance with the anti-HIV assays.

ABBREVIATIONS

AIDS, acquired immunodeficiency syndrome; EC₅₀, the concentration causing 50% inhibition of antiviral activity; CC₅₀, 50% cytotoxicity concentration; DAPY, diarylpyrimidine; NNRTI, non-nucleoside reverse transcriptase inhibitor; NNIBP, NNRTI binding pocket; HAART, highly active antiretroviral therapy; HIV, human immunodeficiency virus; RT, reverse transcriptase; SAR, structure-activity relationship; SI, selection index; WT, wild-type; NVP, nevirapine; DLV, delavirdine; EFV, efavirenz; ETV, etravirine; RPV, rilpivirine; AZT, azidothymidine.

REFERENCES

- (1) Asahchop, E. L.; Wainberg, M. A.; Sloan, R. D.; Tremblay, C. L. Antiviral drug resistance and the need for development of new HIV-1 reverse transcriptase inhibitors. *Antimicrob. Agents. Chemother.* **2012**, 56, 5000–5008.
- (2) Sarafianos, S. G.; Marchand, B.; Das, K.; Himmel, D. M.; Parniak M. A.; Hughes, S. H.; Arnold, E. Structure and function of HIV-1 reverse transcriptase: molecular mechanisms of polymerization and inhibition. *J. Mol. Biol.* **2009**, 385, 693–713.
- (3) Li, D.; Zhan, P.; De Clercq, E.; Liu, X. Strategies for the design of HIV-1 non-nucleoside reverse transcriptase inhibitors: Lessons from the development of seven representative paradigms. *J. Med. Chem.* **2012**, 55, 3595–3613.
- (4) Zhan, P.; Pannecouque, C.; De Clercq, E.; Liu, X. Anti-HIV drug discovery and development: Current innovations and future trends. *J. Med. Chem.* **2016**, 59, 2849–2878.
- (5) Kinch, M. S.; Patridge, E. An analysis of FDA-approved drugs for infectious disease: HIV/AIDS drugs. *Drug Discovery Today.* **2014**, 19, 1510–1513.
- (6) Broder, S. The development of antiretroviral therapy and its impact on the HIV-1/AIDS pandemic. *Antiviral Res.* **2010**, 85, 1–18.

(7) Mehellou, Y.; De Clercq, E. Twenty-six years of anti-HIV drug discovery: where do we stand and where do we go? *J. Med. Chem.* **2010**, 53, 521–538.

(8) Este, J. A.; Cihlar, T. Current status and challenges of antiretroviral research and therapy. *Antiviral Res.* **2010**, 85, 25–33.

(9) Huang, B.; Kang, D.; Yang, J.; Zhan, P.; Liu, X. Novel diarylpyrimidines and diaryltriazines as potent HIV-1 NNRTIs with dramatically improved solubility: a patent evaluation of US20140378443A1. *Expert Opin. Ther. Pat.* **2016**, 26, 281–289.

(10) Iyidogan, P.; Anderson, K. S. Current perspectives on HIV-1 antiretroviral drug resistance. *Viruses.* **2014**, 6, 4095–4139.

(11) Kang, D.; Fang, Z.; Li, Z.; Huang, B.; Zhang, H.; Lu, X.; Xu, H.; Zhou, Z.; Ding, X.; Daelemans, D.; De Clercq, E.; Pannecouque, C.; Zhan, P.; Liu, X. Design, synthesis, and evaluation of thiophene[3,2-d]pyrimidine derivatives as HIV-1 non-nucleoside reverse transcriptase inhibitors with significantly improved drug resistance profiles. *J. Med. Chem.* **2016**, 59, 7991–8007.

(12) Kang, D.; Fang, Z.; Huang, B.; Lu, X.; Zhang, H.; Xu, H.; Huo, Z.; Zhou, Z.; Yu, Z.; Meng, Q.; Wu, G.; Ding, X.; Tian, Y.; Daelemans, D.; De Clercq, E.; Pannecouque, C.; Zhan, P.; Liu, X. Structure-based optimization of thiophene[3,2-d]pyrimidine derivatives as potent HIV-1 non-nucleoside reverse transcriptase inhibitors with improved potency against resistance-associated variants. *J. Med. Chem.* **2017**, 60, 4424–4443.

(13) Kang, D.; Ding, X.; Wu, G.; Huo, Z.; Zhou, Z.; Zhao, T.; Feng, D.; Wang, Z.; Tian, Y.; Daelemans, D.; De Clercq, E.; Pannecouque, C.; Zhan, P.; Liu, X. Discovery of Thiophene[3,2-d]pyrimidine Derivatives as Potent HIV-1 NNRTIs Targeting the Tolerant Region I of NNIBP. *ACS Med. Chem. Lett.* **2017**, 8, 1188–1193.

(14) Kang, D.; Wang, Z.; Zhang, H.; Wu, G.; Zhao, T.; Zhou, Z.; Huo, Z.; Huang, B.; Feng, D.; Ding, X.; Zhang, J.; Zuo, X.; Jing, L.; Luo, W.; Guma, S.; Daelemans, D.; De Clercq, E.; Pannecouque, C.; Zhan, P.; Liu, X. Further Exploring Solvent-Exposed Tolerant

Regions of Allosteric Binding Pocket for Novel HIV-1 NNRTIs Discovery. *ACS Med. Chem. Lett.* **2018**, 9, 370–375.

(15) Tebbe, M. J.; Atton, H. V.; Avery, C.; Bromidge, S. M.; Kerry, M.; Kotey, A. K.; Monck, N. J.; Meniconi, M.; Ridgill, M. P.; Tye, H.; Saiah, E.; Johnsson, K. P.; Gorska, K. I.; Peng, H.; McCall, J. M. Preparation of heteroaryl derivatives as sepiapterin reductase inhibitors. WO2017059191A1 , **2017**.

(16) Sergeyev, S.; Yadav, A. K.; Franck, P.; Michiels, J.; Lewi, P.; Heeres, J.; Vanham, G.; Ariën, K. K.; Vande Velde, C. M.; De Winter, H.; Maes, B. U. 2,6-Di(arylamino)-3-fluoropyridine derivatives as HIV non-nucleoside reverse transcriptase inhibitors. *J. Med. Chem.* **2016**, 59, 1854–1868.

(17) Kertesz, D. J.; Brotherton-Pleiss, C.; Yang, M.; Wang, Z.; Lin, X.; Qiu, Z.; Hirschfeld, D. R.; Gleason, S.; Mirzadegan, T.; Dunten, P. W.; Harris, S. F.; Villasenor, A. G.; Hang, J. Q.; Heilek, G. M.; Klumpp, K. Discovery of piperidin-4-yl-aminopyrimidines as HIV-1 reverse transcriptase inhibitors. N-benzyl derivatives with broad potency against resistant mutant viruses. *Bioorg. Med. Chem. Lett.* **2010**, 20, 4215–4218.

(18) Lansdon, E. B.; Brendza, K. M.; Hung, M.; Wang, R.; Mukund, S.; Jin, D.; Birkus, G.; Kutty, N.; Liu, X. Crystal structures of HIV-1 reverse transcriptase with etravirine (TMC125) and rilpivirine (TMC278): implications for drug design. *J. Med. Chem.* **2010**, 53, 4295–4299.

(19) Pauwels, R.; Balzarini, J.; Baba, M.; Snoeck, R.; Schols, D.; Herdewijn, P.; Desmyter, J.; De Clercq, E. Rapid and automated tetrazolium-based colorimetric assay for the detection of anti-HIV compounds. *J. Virol. Methods* **1988**, 20, 309–321.

(20) Pannecouque, C.; Daelemans, D.; De Clercq, E. Tetrazoliumbased colorimetric assay for the detection of HIV replication inhibitors: revisited 20 years later. *Nat. Protoc.* **2008**, 3, 427–434.

(21) Sun, L. Q.; Zhu, L.; Qian, K.; Qin, B.; Huang, L.; Chen, C. H.; Lee, K. H.; Xie, L. Design, synthesis, and preclinical evaluations of novel 4-substituted 1,5-diarylanilines as

potent HIV-1 non-nucleoside reverse transcriptase inhibitor (NNRTI) drug candidates. *J. Med. Chem.* **2012**, 55, 7219–7229.